

# Electronic Supplementary Material for Physical Chemistry Chemical Physics

The top and side views, monolayer-resolved band structures for six different stacking configurations of the  $\alpha$ -Te/GaAs and  $\gamma$ -Te/GaAs vdWH are depicted in Figs. S1-S4, and the Fig. S5 depicts the monolayer-resolved band structures of the  $\alpha$ -Te/GaAs and  $\gamma$ -Te/GaAs vdWHs based on the hybrid functional HSE06 method. Furthermore, the three-dimensional plane-averaged charge density difference along the  $z$ -axis direction of the  $\alpha$ -Te/GaAs and  $\gamma$ -Te/GaAs vdWHs is illustrated in Fig. S6. Wherever, the photon energy dependent optical reflection coefficients of the  $\alpha$ -Te/GaAs and  $\gamma$ -Te/GaAs vdWH under the 6%, -3%, 0%, 3%, and 6% biaxial strains are demonstrated in Fig. S7, and one observes the photon energy dependent optical absorption and transmission coefficients of the  $\alpha$ -Te/GaAs and  $\gamma$ -Te/GaAs vdWHs in Fig. S8 based on the hybrid functional HSE06 method.

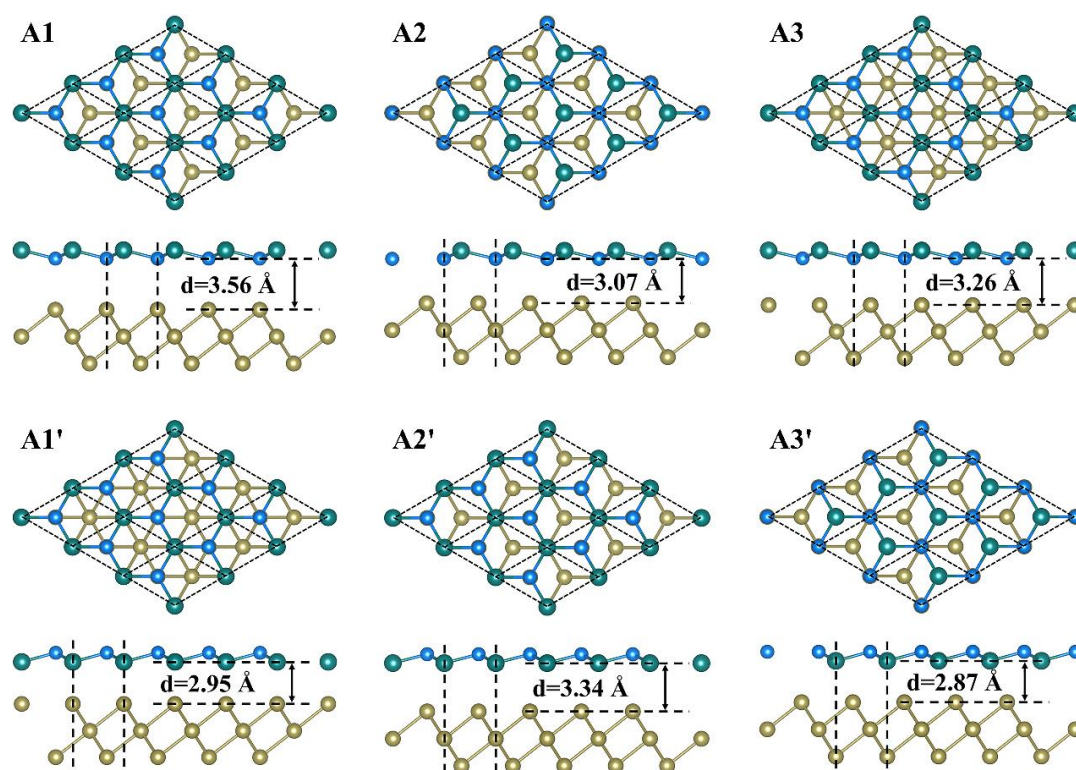


Fig. S1. Top and side views for six different stacking configurations of the  $\alpha$ -Te/GaAs vdWH.

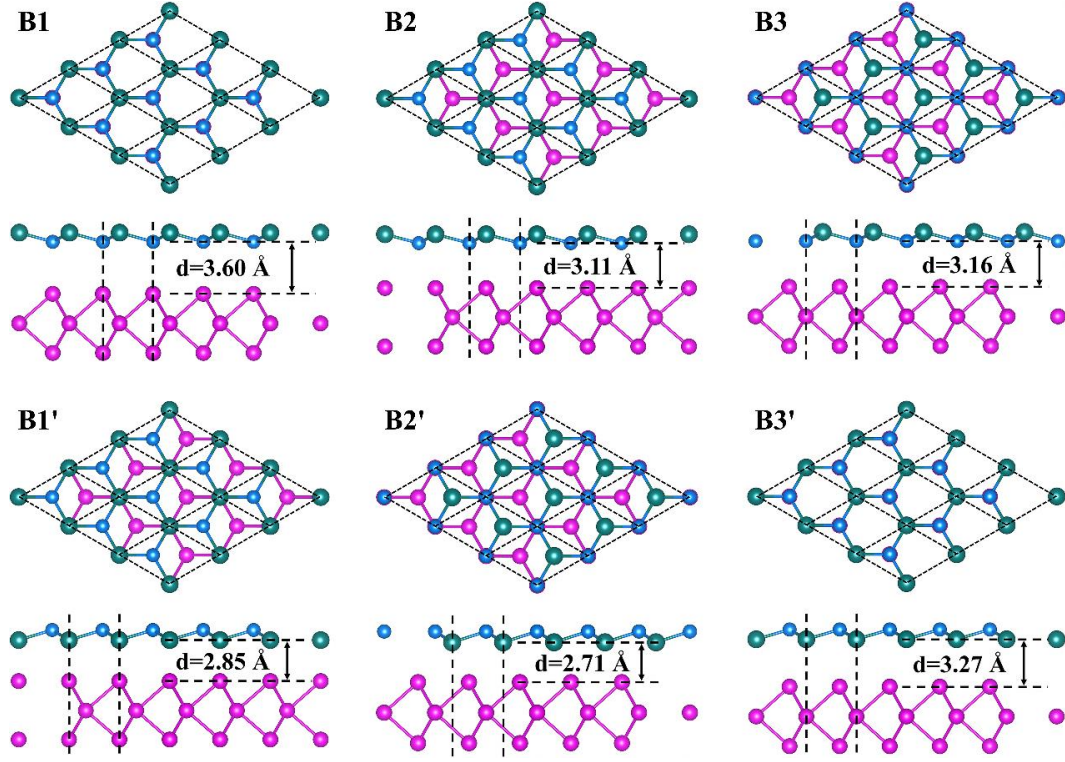


Fig. S2. Top and side views for six different stacking configurations of the  $\gamma$ -Te/GaAs vdWH.

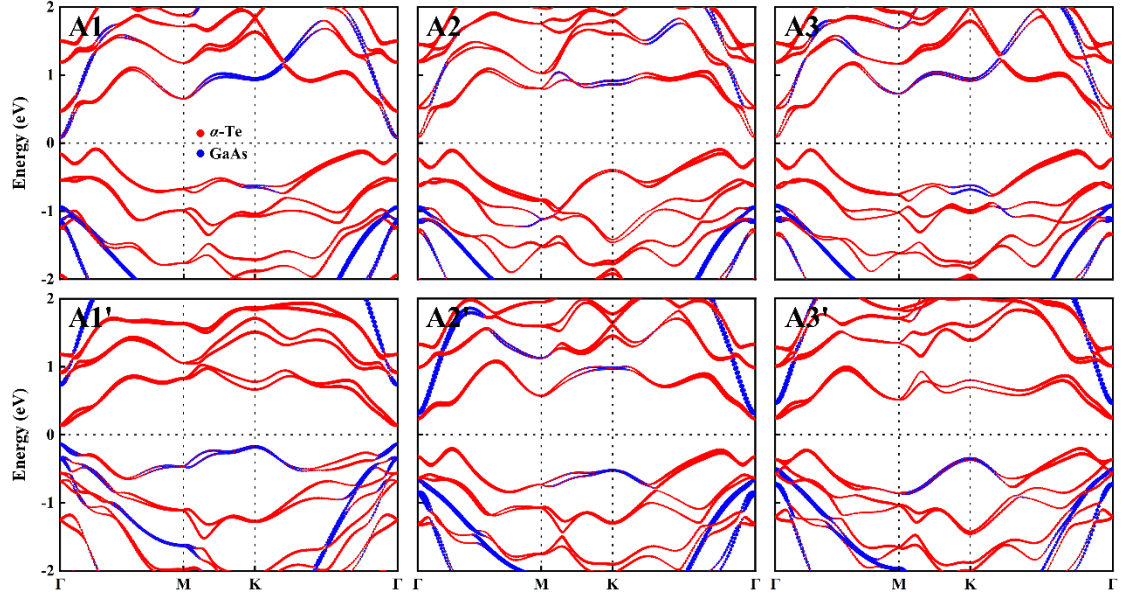


Fig. S3. Monolayer-resolved band structures for six different stacking configurations of the  $\alpha$ -Te/GaAs vdWH, where the red and blue components represent the contributions of  $\alpha$ -Te and GaAs monolayers, respectively.

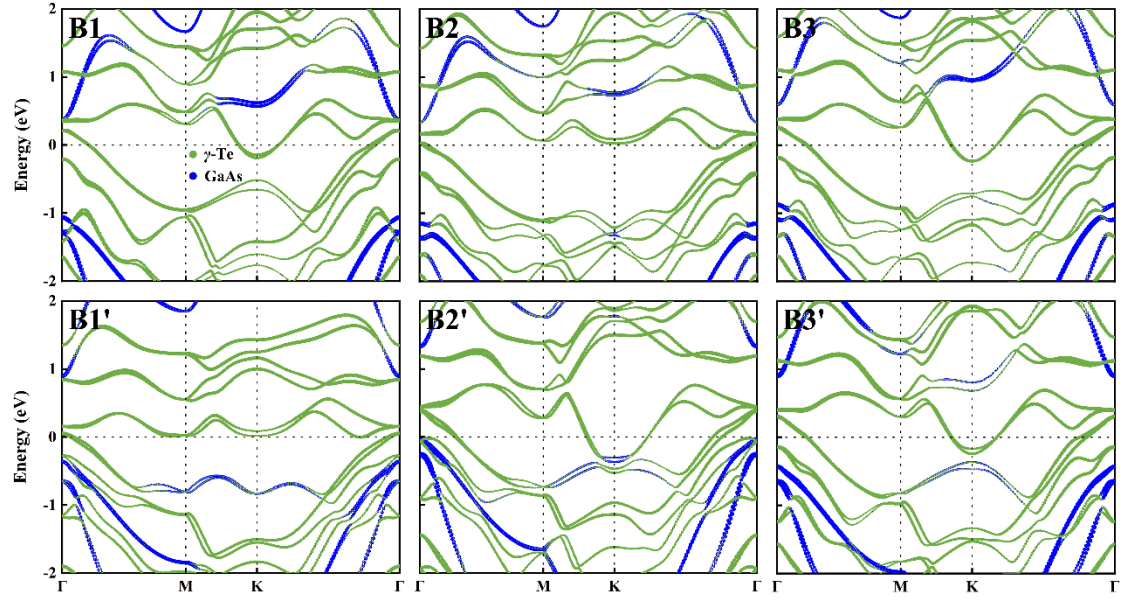


Fig. S4. Monolayer-resolved band structures for six different stacking configurations of the  $\gamma$ -Te/GaAs vdWH, where the green and blue components represent the contributions of  $\gamma$ -Te and GaAs monolayers, respectively.

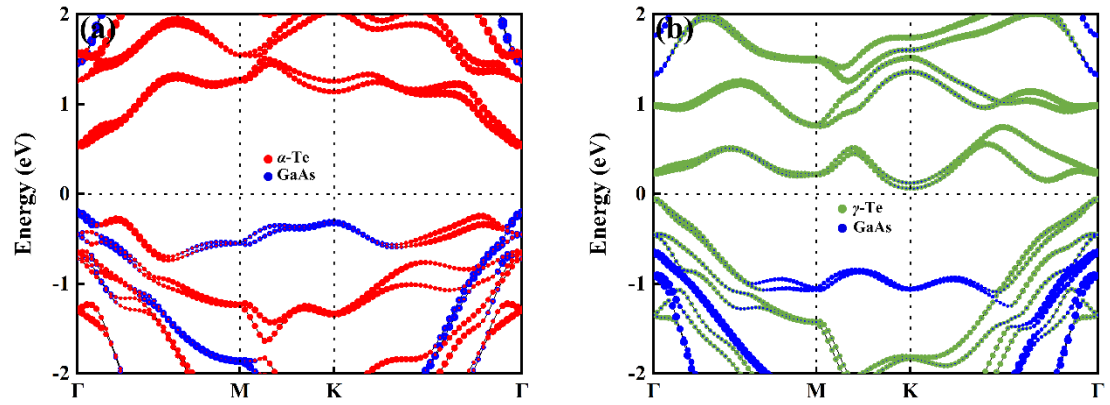


Fig. S5. Monolayer-resolved band structures of the  $\alpha$ -Te/GaAs (a) and  $\gamma$ -Te/GaAs (b) vdWHs based on the hybrid functional HSE06 method.

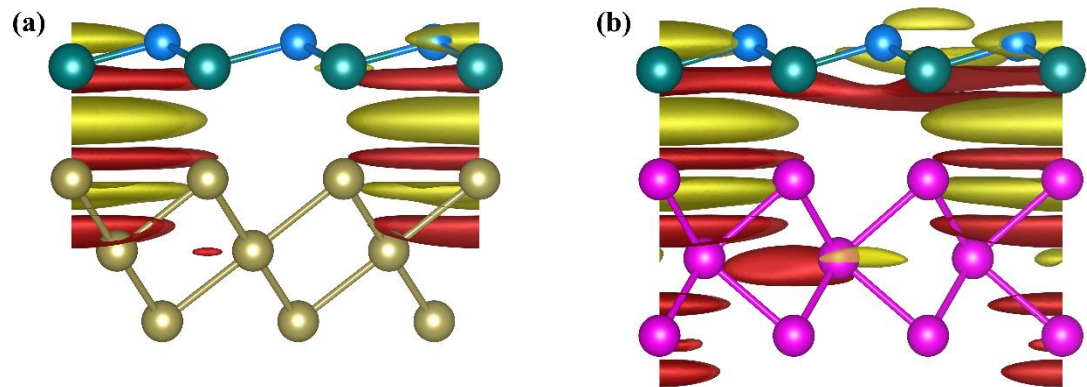


Fig. S6. Three-dimensional plane-averaged charge density difference along the z-axis direction of the  $\alpha$ -Te/GaAs (a) and  $\gamma$ -Te/GaAs (b) vdWH, where the red and yellow regions denote the losing and gaining of electrons, respectively.

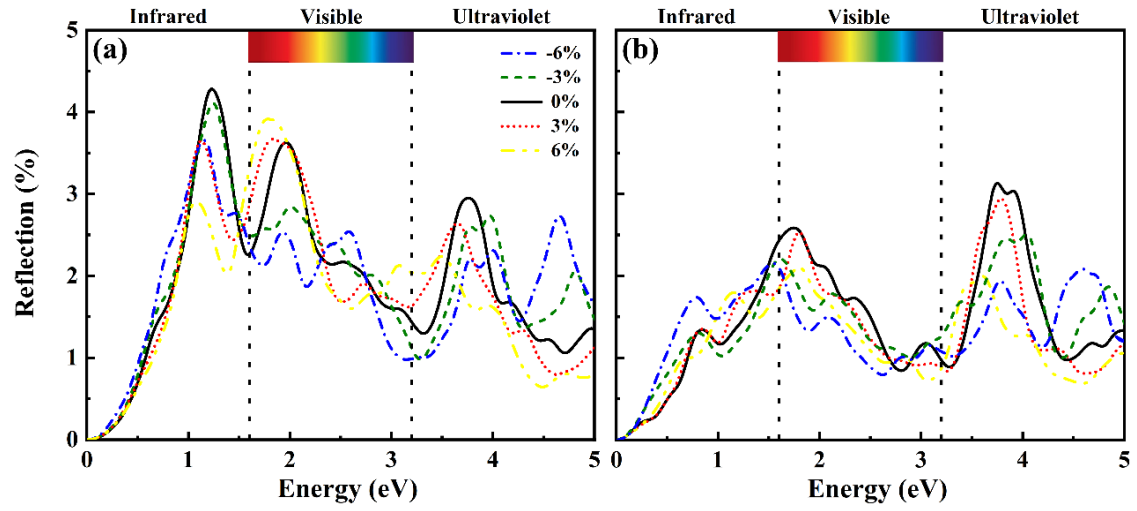


Fig. S7. Photon energy dependent optical reflection coefficients of the  $\alpha$ -Te/GaAs (a) and  $\gamma$ -Te/GaAs (b) vdWHs under the -6%, -3%, 0%, 3%, and 6% biaxial strains, where the blue dashed-dot line, olive green dashed line, black solid line, red dotted line, and yellow double-dashed-dot line indicate the light absorption and transmission coefficients under the biaxial strains of -6%, -3%, 0%, 3%, and 6%, respectively.

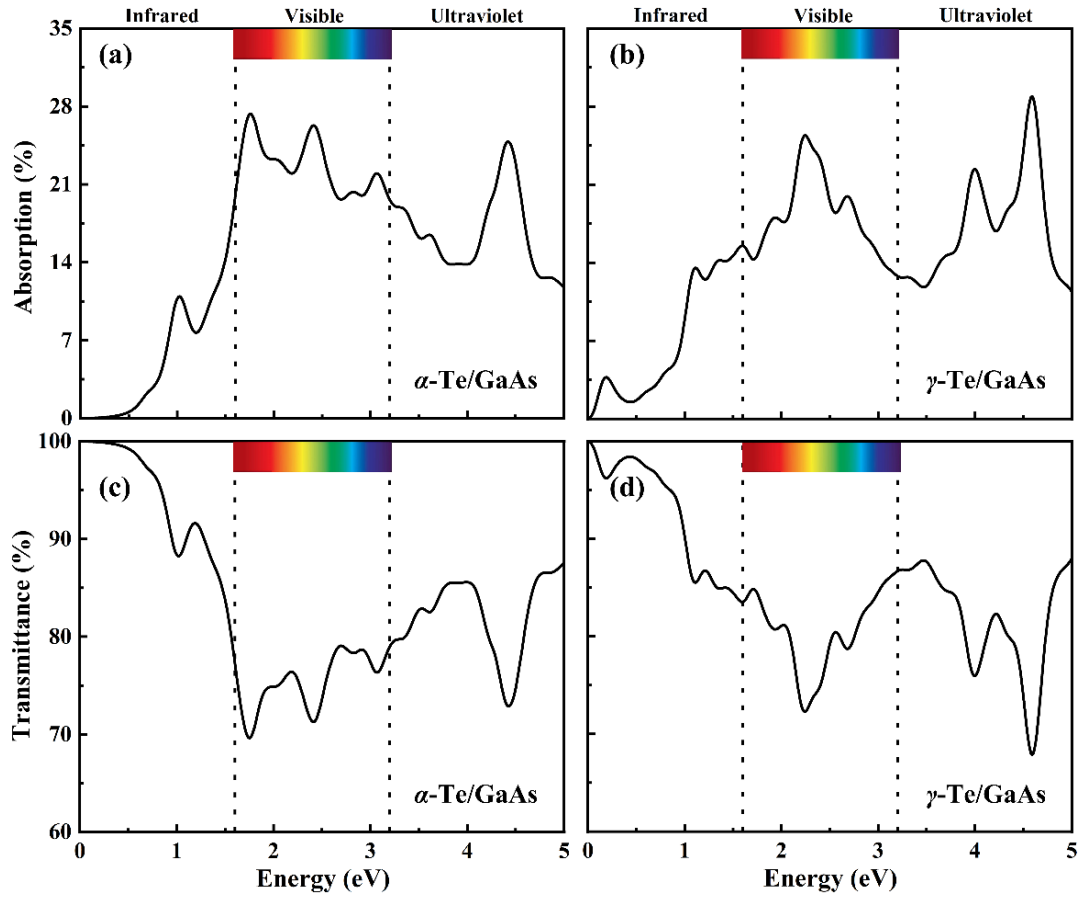


Fig. S8. Photon energy dependent optical absorption (a)-(b) and transmission (c)-(d) coefficients of the  $\alpha$ -Te/GaAs and  $\gamma$ -Te/GaAs vdWHs based on the hybrid functional HSE06 method.